Local structure about Mn atoms in $In_{1-x}Mn_xAs$ diluted magnetic semiconductors

A. Krol, Y. L. Soo, S. Huang, Z. H. Ming, and Y. H. Kao
Department of Physics, State University of New York at Buffalo, Buffalo, New York 14260

H. Munekata and L. L. Chang
IBM Research Division, Thomas J. Watson Research Center, P. O. Box 218, Yorktown Heights, New York 10598

(Received 8 June 1992; revised manuscript received 30 November 1992)

X-ray-absorption fine-structure measurements were performed at the Mn K edge on $In_{0.88}Mn_{0.12}As$ diluted magnetic semiconductors prepared by molecular-beam epitaxy. It has been found that in the high-growth-temperature samples ($T_s=280$ °C), Mn atoms are primarily incorporated in the form of MnAs clusters with NiAs structure. No significant disorder is observed. In the low-growth-temperature samples ($T_s=210$ °C), the majority of Mn atoms form small ($r\sim3$ Å), disordered, sixfold-coordinated centers with As. The presence of disorder in MnAs centers for the latter case is established using the method of cumulants. Only a very small fraction of Mn atoms may substitute for In in the zinc-blende InAs structure. Effective valency and coordination of Mn atoms deduced from the near-edge structure are the same for both the high- and low-growth-temperature $In_{1-x}Mn_xAs$ films. The formal valency is lower than +3. The local structures established in the present work are consistent with the observed difference in magnetic behavior for samples prepared at different substrate temperatures.

I. INTRODUCTION

III-V diluted magnetic semiconductors have been synthesized by incorporating a large amount of Mn into InAs during molecular-beam epitaxy (MBE).[1-5] It has been found that physical properties of these nominal $In_{1-x}Mn_xAs$ alloys strongly depend on growth conditions. X-ray diffraction as well as magnetic studies indicate that all the films grown at low substrate temperatures around 200 °C on GaAs(100) behave primarily as a homogeneous, paramagnetic alloy. This phase has been confirmed with Mn composition up to $x\simeq0.2$. On the other hand, samples grown at a substrate temperature around 300 °C with relatively high Mn compositions ($x>0.03$) exhibit ferromagnetic behavior, from which the presence of MnAs clusters has been suggested.

In light of such sensitive dependence of physical properties on growth conditions (Mn concentration and substrate temperature), local structures around Mn atoms are believed to vary and thus play a pivotal role in this new alloy semiconductor. In this paper, x-ray-absorption fine-structure (XAFS) measurements are carried out to probe the local environment surrounding the Mn atoms in $In_{1-x}Mn_xAs$ films grown at two different substrate temperatures $T_s=210$ and 280 °C.

II. SAMPLES AND ANALYSES

A. Experiment

Films of $In_{0.88}Mn_{0.12}As$ with 2.5-μm thickness were grown by the MBE method at two different substrate temperatures $T_s=210$ and 280 °C on InAs(0.05 μm)/GaAs(0.3 μm)/GaAs(100) substrates. In both films, the Auger depth profile indicated the lack of gross atomic segregation.[5] The model compound of 1-μm-thick polycrystalline MnAs film was also prepared by MBE on the InAs/GaAs(100) surface at $T_s=200$ °C.

X-ray-absorption fine-structure (XAFS) measurements were performed on two $In_{0.88}Mn_{0.12}As$ samples ($T_s=210$ and 280 °C). The XAFS spectra, obtained in fluorescence mode at the National Synchrotron Light Source at the X3B1 beamline, were measured at the Mn K edge at both room temperature and 110 K. An energy dispersive solid-state Si(Li) detector, with an energy resolution of 165 eV at the Mn K edge, was used to collect the Mn $K\alpha$ photons. A nitrogen-filled gas detector was used as a beam monitor. In order to minimize the harmonic content, the double-crystal monochromator equipped with Si(111) crystals was detuned to 50% of the fundamental intensity. The 0.25-mm slits in the vertical dimension were used to define the x-ray beam. The resolution of the monochromator is estimated to be ~3 eV at the Mn K edge. Counts of over 10^6 effective photons per energy point were accumulated by taking multiple scans.

B. XAFS data analysis

The XAFS data were analyzed by means of standard methods.[6,7] The fluorescence data obtained in the experiment were corrected at first for the thickness effects[6,7] using photoabsorption data published by Henke *et al.*[8] The energy dependence in the beam monitor was corrected also using data published by Henke *et al.*[8] In the second stage of data reduction, the preedge background was subtracted, and subsequently the atomiclike background above the Mn K edge was simulated by means of a cubic spline with two nodes. An energy derivative of the background absorption vs k was examined in order to select its smooth energy dependence without the XAFS-originated oscillations. The Mn K edge value was assumed to be at the absorption threshold at $E_0=6545$ eV for both of the $In_{0.88}Mn_{0.12}As$ films and $E_0=6547$ eV for the polycrystalline MnAs model compound, and these energies were used to calculate k values. All spectra were

normalized to the edge step at a properly chosen energy of $E_i = 6575$ eV. The following criteria were used for the selection of this energy value: (i) its position on the node of $d\mu(E)/dE$ and (ii) its position on the background absorption curve $\mu_b(E)$. The XAFS interference function is defined as $\chi(k) = [\mu(k) - \mu_b(k)]/\mu_i$, with the photoelectron wave vector given by $k = [2m(E - E_0)]^{1/2}/\hbar$; where μ_i is the absorption coefficient at the normalization point E_i, $\mu_b(k)$ is the smooth atomiclike background, and $\mu(k)$ is the experimentally obtained and corrected absorption

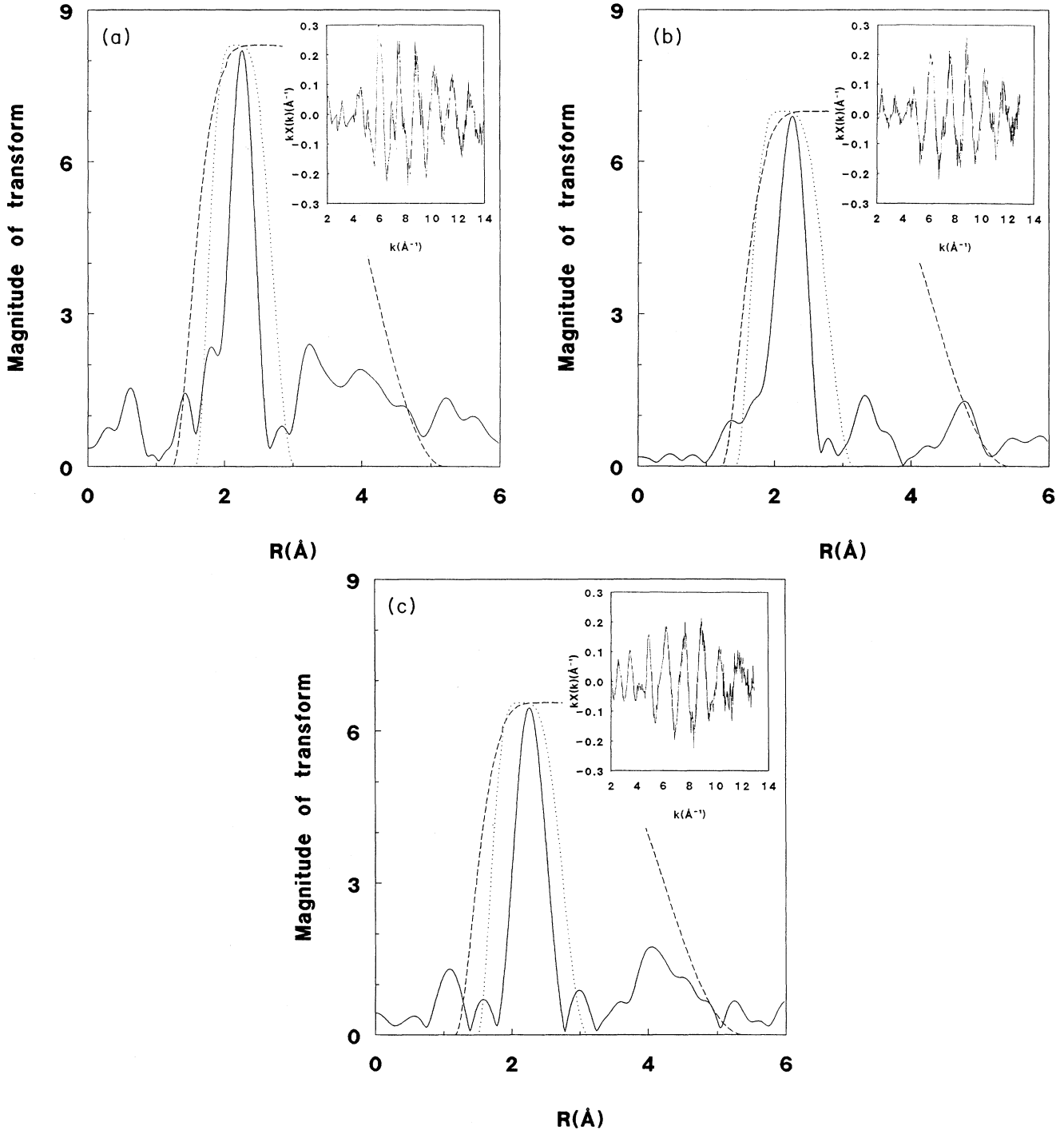

FIG. 1. Magnitude of the Fourier transform of $k\chi_c(k)$ and two different windows w_1 (broken line) and w_2 (dotted line) used for spectral isolation of the near-neighbor shells. The corrected XAFS functions $k\chi_c(k)$ are shown in the insets. (a) The MnAs film with NiAs structure. (b) The $In_{0.88}Mn_{0.12}As$ film grown at 280 °C substrate temperature. (c) The $In_{0.88}Mn_{0.12}As$ film grown at 210 °C substrate temperature.

TABLE I. (a) Environment about In in InAs. (b) Environment about Mn in MnAs.

Central atom	Neighboring atoms	Radial distance (Å)	Number of neighbors
	(a)		
In	As	2.620	4
In	In	4.278	12
In	As	5.017	12
	(b)		
Mn	As	2.571	6
Mn	Mn	2.845	2
Mn	Mn	3.710	6
Mn	As	4.514	6
Mn	Mn	4.676	12
Mn	As	4.776	6

coefficient. The $\chi(k)$ function was then normalized to the photoabsorption cross-section jump by multiplying a factor $\mu_{Mn}(E_0)/\mu_{Mn}(E)$, where $\mu_{Mn}(E)$ is the photoabsorption coefficient due to free manganese atoms only, calculated by using tables published by Henke *et al.*[8] The weighted and corrected XAFS function $k\chi_c(k)$ thus obtained for the MnAs sample and the $T_s=280$ and 210 °C $In_{0.88}Mn_{0.12}As$ films are shown in the insets in Figs. 1(a), 1(b), and 1(c), respectively.

The next step in the analysis consisted of fast Fourier transformation of the $k\chi_c(k)$ data to the r space (see Fig. 1), followed by the spectral isolation of the contributions from the shells close to ($r \leq 3$ Å) and more distant from ($3 \leq r \leq 5$ Å) the central x-ray-absorbing manganese atom. This was accomplished by means of the functions shown in Fig. 1, which were used as windows to transform the data back to the k space.

The fundamental differences between cation environment in zinc blende vs NiAs structure (see Table I) were utilized in this work to determine the local structure about manganese atoms in the investigated $In_{1-x}Mn_xAs$ samples. In the zinc-blende structure InAs, the nearest-neighbor shell around an In atom consists of four As atoms at 2.62 Å, and the second-neighbor shell has a 4.278-Å radius with 12 In atoms. On the other hand, the NiAs structure is one of the stable phases of crystalline MnAs, where a Mn atom has the nearest-neighbor shell with six As atoms at 2.571 Å, and two Mn atoms in the second-neighbor shell at 2.845 Å. The third-neighbor shell consists of six Mn atoms at 3.71 Å.

A nonlinear least-squares fitting was applied to the filtered k-space data. The amplitude and phase functions were taken from tables published by McKale *et al.*[9] The Fourier-transform resolution has a restricting effect on the number of degrees of freedom allowed by the filtering process which is defined by the filter width ΔR. The number of independent variables which may be fitted can be estimated as

$$N_{\text{free}} \simeq \frac{2\Delta R\,\Delta k}{\pi}, \tag{1}$$

where $\Delta k = k_{\max} - k_{\min}$ is the range of data in k space.[6] The value of $N_{\text{free}} \leq 10$ has been obtained from the k ranges of our data and the width of filters used in the near-shells analysis.

III. RESULTS AND DISCUSSION

A. Near-shells analysis

1. *MnAs*

The MnAs model compound XAFS data obtained at 110 K were first fitted assuming small Gaussian disorder and no significant multiple-scattering effects. The window function extends from 1.6 to 3.0 Å [see dotted curve in Fig. 1(a)]. Based on the results of x-ray-diffraction (XRD) analysis obtained for this sample, the NiAs crystallographic structure was assumed.[10] Thus the variables in the fitting procedure were only the photoelectron inelastic loss factors, Debye-Waller factors, and energy origins for each single shell. In the initial analysis a one-shell model was first applied, so that the contribution from the Mn second-neighbor shell (two Mn atoms) was neglected. A reasonably good fit was achieved [see the dotted curve in Fig. 2(a) and Table II], thus proving that the nearest-neighbor-shell dominates the XAFS spectra.

The inclusion of the Mn second-neighbor shell further improved the goodness of the fit by a factor of 2.3. As expected, the differences between one- and two-shell models are more pronounced in the small-k regime below 7 $Å^{-1}$ [see the solid line in Fig. 2(a)]. One can see that in this region the two-shell model has the amplitude and phase in better agreement with the experiment than the one-shell model. One can conclude that structural information on the second shell can be inferred from the experimental XAFS data.

The transferability of the inelastic loss factors was assumed, and the loss factors obtained for the model compound were subsequently used in the fitting of the $In_{x-1}Mn_xAs$ XAFS data. The possible k dependence of the loss factors was neglected.

2. *High-growth-temperature $In_{1-x}Mn_x$ As*

The high-growth-temperature ($T_s=280$ °C) film XAFS data obtained at 110 K were first analyzed using an iden-

tical procedure to that for MnAs, i.e., assuming small Gaussian disorder and no significant multiple-scattering effects. The variables in the fitting procedure were distances, coordination numbers, and Debye-Waller factors. The inelastic loss factors were obtained from the model-compound fit. Again the one-shell model was first employed, resulting in a satisfactory fit [see the dotted curve in Fig. 2(b) and Table II]. The striking feature of the obtained parameters is that they closely resemble the parameters characteristic of environment around the Mn atoms as in MnAs but with the Mn-As distance reduced to 2.55 ± 0.01 Å, and σ in the Debye-Waller factor increased to 0.05 ± 0.04 Å. The quality of the fit was improved upon expansion of the model by allowing for the presence of two Mn atoms in the second shell. The parameters obtained with this two-shell fit confirmed the ex-

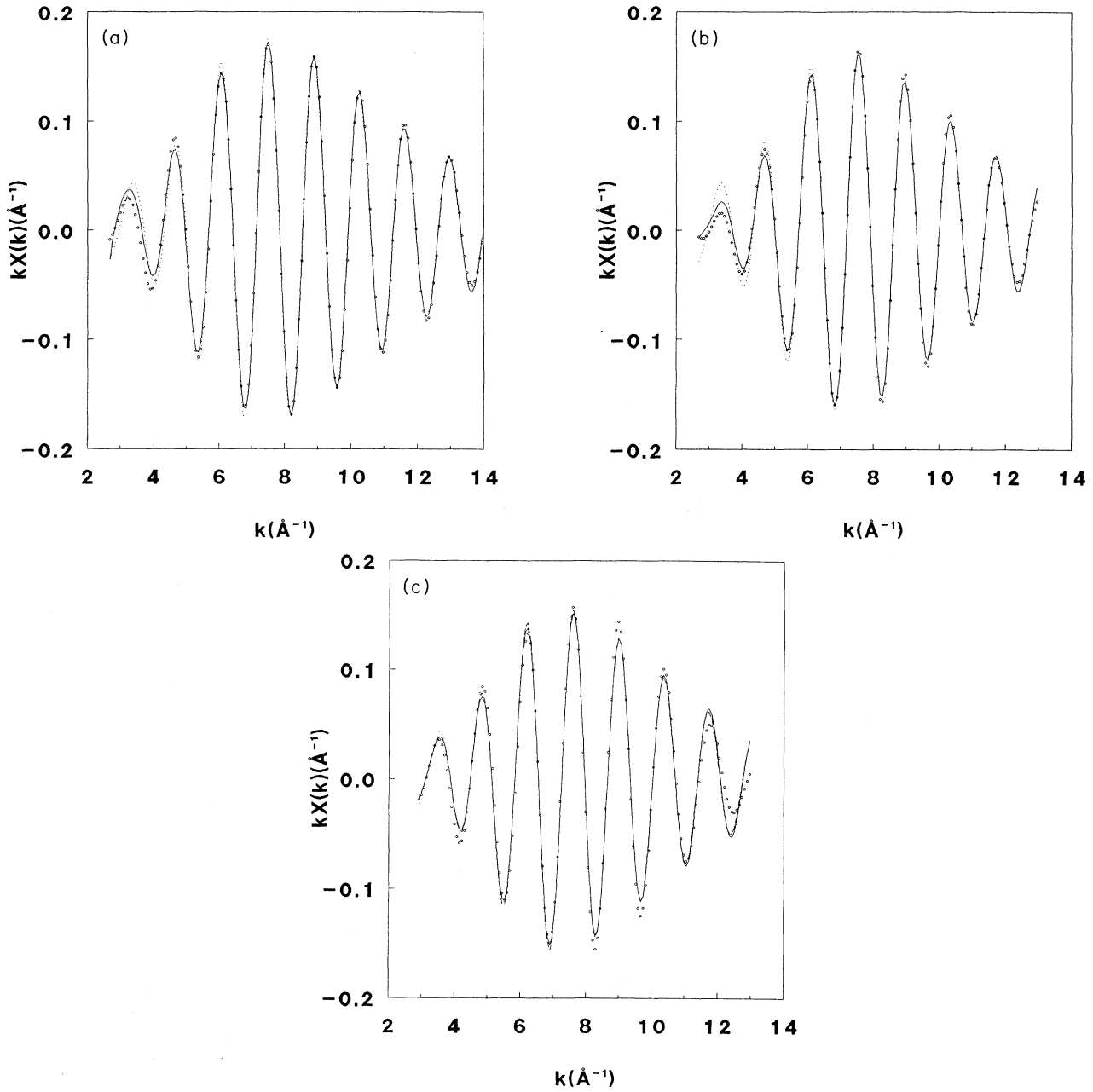

FIG. 2. The least-squares fit of $k\chi_c(k)$ experimental data (open circles) for near-neighbor shells about Mn obtained under the assumption that only small disorder with a Gaussian pair distribution function is present. (a) The MnAs film with NiAs structure. (b) The $In_{0.88}Mn_{0.12}As$ film grown at 280 °C substrate temperature. Dotted line: one-shell fit; solid line: two-shell fit. (c) The $In_{0.88}Mn_{0.12}As$ film grown at 210 °C substrate temperature. Dotted line: one-shell fit; broken line: two-shell fit; solid line: three-shell fit.

istence of the Mn shell in the NiAs-like environment of the central Mn atom.

No satisfactory fit could be obtained if all the Mn atoms are assumed to be fourfold coordinated with As atoms as in the zinc-blende InAs structure with an interatomic distance around 2.55–2.62 Å (i.e., substitution of all the available Mn for the In sites). This finding indicates that the majority of manganese atoms in this sample is in the NiAs-like phase.

We have also examined as to whether a trace of substitution-type Mn can be extracted from the XAFS data. To study this, it was assumed that a fraction p of manganese atoms substitute for In in the zinc-blende phase, thus forming an alloy. In this analysis, the calculated k dependence of the XAFS spectra is represented by a linear combination of those due to sixfold- and fourfold-coordinated Mn atoms, so that the relative fractional occupation parameter p is a fitted parameter. Consequently $p \sim (10 \pm 10)\%$ was obtained. However, the goodness of fit worsened by $\sim 30\%$ as compared to that obtained for the two-shell model (see Table II).

In view of the fact that a global minimum is reached for the two-shell NiAs-like short-range order (SRO), the model with the NiAs-like environment about all Mn atoms describes the experimental data better than a three-shell model, which allows for tetrahedral coordination of some Mn atoms. This result again suggests that practically all the Mn atoms detected are in the form of MnAs clusters.

3. *Low-growth-temperature $In_{1-x}Mn_x$ As*

The low-growth-temperature ($T_s = 210\,^\circ$C) $In_{1-x}Mn_xAs$ film XAFS data obtained at 100 K were also analyzed using an identical procedure to that for MnAs, i.e., assuming small Gaussian disorder and no significant multiple-scattering effects. The one-shell model with either NiAs or zinc-blende structure was first employed. Once again, no satisfactory fit could be obtained if all the Mn atoms were assumed to be fourfold coordinated with As atoms, as in the pure zinc-blende InAs phase, whereas an adequate fit to the experimental data with Mn sixfold coordinated with As atoms was obtained in the k region below 11 $Å^{-1}$. Contrary to the situation observed for the MnAs and high-growth-temperature $In_{1-x}Mn_xAs$ samples, the one-shell model provides a seemingly adequate description of the experimental data in the k region below 5 $Å^{-1}$. The extracted Mn-As bond length was 2.56 Å. As mentioned before, behavior of the $\chi(k)$ function in the low-k region is especially sensitive to the presence of next-neighbor shells. On the other hand, the one-shell model gave rise to a much poorer fit to the data at larger k than that found in the two previous cases. One notes an increasing discrepancy in the amplitude and phase between the data and the fit with increasing photoelectron wave vector k. The relative amplitude discrepancy reaches as much as $\sim 80\%$ for $k > 12$ $Å^{-1}$. This problem was also noticeable in the modeling of the high-growth-temperature $In_{1-x}Mn_xAs$ film $\chi(k)$ function, but there the relative amplitude discrepancy only reached $\sim 10\%$ for $k > 12$ $Å^{-1}$. Within the context of the Gaussian approximation, the parameters obtained indicate the sixfold coordination of the majority of Mn, similar to the high-growth-temperature $In_{1-x}Mn_xAs$, but with a Mn-As distance changed to 2.56 ± 0.05 Å, and σ in the Debye-Waller factor increased to 0.06 ± 0.4 Å.

The quality of fit in the small-k regime was somehow

TABLE II. Curve-fitting results with a model assuming small Gaussian disorder. The distances R are in units of Å. σ^2 in the Debye-Waller factors are in units of 10^{-3} $Å^2$. N denotes the number of neighbors in a given shell. p is the relative fractional occupation parameter. Central atom: Mn. R and N values were fixed for MnAs. F.E. means fit errors. E.E. means estimated experimental errors.

	Neighboring shells										
	As(NiAs-like)			Mn(NiAs-like)			As(zinc blende)				Residual
	R	N	σ^2	R	N	σ^2	R	N	σ^2	p	($\times 10^{-3}$)
MnAs											
	2.571	6.0	1.7								14.3
	2.571	6.0	1.6	2.845	2.0	20.7					6.1
F.E.			0.5			36.0					
E.E.	0.01	1.4	0.9	0.10	2.0	40.0					
$In_{1-x}Mn_xAs$		$T_s = 280\,^\circ$C									
	2.55	6.2	2.8								9.5
	2.55	6.2	2.8	2.86	2.3	31.7					3.6
	2.55	6.2	2.2	2.88	2.3	30.3	2.63	4.3	1.0	0.10	4.7
F.E.	0.01	1.3	1.5	0.10	2.0	45.0	0.06	4.0	7.0	0.10	
E.E.	0.01	1.4	1.3	0.10	2.0	60.0	0.10	1.0	8.0	0.10	
$In_{1-x}Mn_xAs$		$T_s = 210\,^\circ$C									
	2.56	6.2	3.2								17.6
	2.56	6.2	3.2	2.80	2.3	87.7					17.1
	2.55	6.2	2.0	2.80	2.3	92.6	2.64	4.2	1.2	0.18	16.8
F.E.	0.05	2.0	2.0	0.5	3.0	60.0	0.08	3.0	7.0	0.15	
E.E.	0.01	1.4	1.3	0.10	2.0	90.0	0.10	1.0	8.0	0.10	

improved (by ~3%) upon extension of the model to include also two Mn atoms in the second shell. The apparent Mn-Mn distance was reduced to 2.80±0.5 Å, and the fitted Debye-Waller factor was extremely high (a factor of 3 higher) as compared to those of the high-growth-temperature sample. However, these values cannot be trusted due to insufficient improvements (lowering) of the residual value of the fit. Upon assuming that some fraction p of manganese atoms substitutes for In in the zinc-blende phase, an insignificant improvement (by 2%) in the small-k regime was found and a global minimum of the fit was reached. The obtained relative fractional occupation parameter $p=(18\pm15)\%$, with a Mn-As nearest-neighbor distance of 2.64±0.08 Å, may indicate that in this sample a small fraction of Mn probably is fourfold coordinated in the $In_{1-x}Mn_xAs$ alloy (see Table II). However, the confidence level of the obtained parameters is very low due to poor fit quality at higher k ($k>11$ Å).

We note that the extension from the one-shell model to the two- or three-shell model has not influenced the calculated $\chi(k)$ function sufficiently to improve the fit in the high-k region. A shifted distance, an increase in the apparent Debye-Waller factor, and an increasing discrepancy between the fit and experiment with increasing k, all indicate the typical "symptoms" of the presence of asymmetrical pair distribution when fitted with a Gaussian peak.[6,11,12] Thus one can conclude that a possible reason for the difficulties experienced in the fitting of the XAFS data for the low-growth-temperature sample is due to the fact that an inadequate pair distribution function was assumed. This possibility is further discussed in the next section. The results obtained by assuming a Gaussian pair distribution function can only be viewed as a first-order approximation.

B. Presence of large disorder

1. General test of the existence of disorder

First we have tested our data for the presence of asymmetry in the pair distribution function. To this end, the complex transform in the following form was taken:

$$\phi(r)=\int_{k_{\min}}^{k_{\max}} k\chi_c(k)e^{i2kr}\frac{e^{-i\delta(k)}}{Env(k)}w(k)dk \ , \qquad (2)$$

where $Env(k)$ is the XAFS amplitude, $w(k)$ is a window function, and $\delta(k)$ is the total XAFS phase shift.[12] Theoretical values obtained from McKale's tables were used for the present case.[9] Due to the dominance of the nearest-neighbor shell in the analyzed XAFS spectra, a one-shell approximation in a multishell system is justified in the above test of the presence of disorder. A significant separation of 0.009 Å of the peaks in $-\mathrm{Im}\phi$ and $|\phi|$ was detected for the low-growth-temperature sample, confirming the presence of asymmetry in the pair distribution function. For the MnAs and high-growth-temperature sample the observed separations were only 0.003 and 0.004 Å, respectively. As was mentioned before, the presence of asymmetry in the low-growth-temperature sample is also evidenced at large k by the incorrect phase and amplitude of the fitted XAFS function in the Gaussian approximation [see Fig. 2(c)]. On the other hand, for the high-growth-temperature film and the MnAs compound [see Figs. 2(a) and 2(b)] the Gaussian approximation was sufficient to achieve a good fit in the equivalent whole range used in the k space.

2. Cumulant expansion

In the XAFS analysis with large disorder, a fit of the coefficients in cumulant expansion[13] was performed. The filtered XAFS function was fitted in the k space in order to obtain C_{2j}, C_{3j}, and C_{4j} cumulants for the jth shell. The even cumulants contribute to a correction in the XAFS amplitude only, while the odd cumulants are effective only in the XAFS phase, assuming that the photoelectron mean free path is independent of k. One should note that the cumulant expansion is expected to break down for higher k and the parameters obtained may have large errors (i.e., larger than the expected least-squares-fit errors) especially in the case of large disorder.[11] We addressed this problem by performing the fit using a variable upper limit in the k space. Only weak dependence of the obtained cumulants on the k range was observed.

Another problem is the number of adjustable parameters which, upon introducing the cumulant coefficients, increases by two for every shell. Since the number of degrees of freedom allowed by our XAFS data (defined by the window used in k and r space) is $N_{\text{free}}\leq 10$, reasonable fits can only be achieved under some restricted conditions. Based on the results obtained using a small disorder approximation, we have assumed that only the sixfold-coordinated centers are involved in the XAFS data, and coordination numbers were fixed with values characteristic of the NiAs structure [Table I(b)], thus limiting the number of adjustable parameters to below 10.

First the one-shell model was fitted. The results are collected in Table III. An improvement of the fit as compared to that of the small disorder model was achieved only for the low-growth-temperature $In_{1-x}Mn_xAs$ sample in the high-k range [compare Fig. 2(c) with Fig. 3(c)]. The obtained high values of C_3 and C_4 parameters in the sixfold-coordinated As shell in this sample are consistent with the conclusion reached before of high disorder in the Mn-As bonds in the MnAs centers in this material. In the high-growth-temperature $In_{1-x}Mn_xAs$ film, moderate values of C_3 and C_4 cumulants were obtained, allowing for moderate disorder of these bonds. However, the residual value of the fit became ~10% larger than that of the value reached in the small disorder approximation. This is mainly caused by using a fixed coordination number parameter during the fit. The MnAs compound does not exhibit any significant disorder, i.e., the obtained higher cumulants are very small.

In general, the two-shell model gives rise to improvement of fits in the small-k regime; however, one should note the large fit errors characteristic of the two-Mn shell at 2.83–2.845 Å. For the MnAs model compound, the fitted values of the cumulant expansion coefficients relevant to the two-Mn shell are negligibly small (see Table III), thus confirming the applicability of the small

Gaussian disorder approximation to the XAFS data obtained for this sample. For the high-growth-temperature sample, comparable to that of the MnAs model, values of the C_3 and C_4 effective distribution cumulants are obtained with only the C_2 cumulant being somehow larger. This reconfirms that only small disorder is present in the two-Mn shell in this sample (see Table III). The situation is quite different for the low-growth-temperature sample. In this case, the inclusion of the two-Mn shell results in a very high value of the C_3 cumulant, which is an order of magnitude larger than that of the MnAs model compound (see Table III). This clearly establishes the presence of large disorder in the Mn-Mn bonds. In light of these results, the fit in the high-k regime should be im-

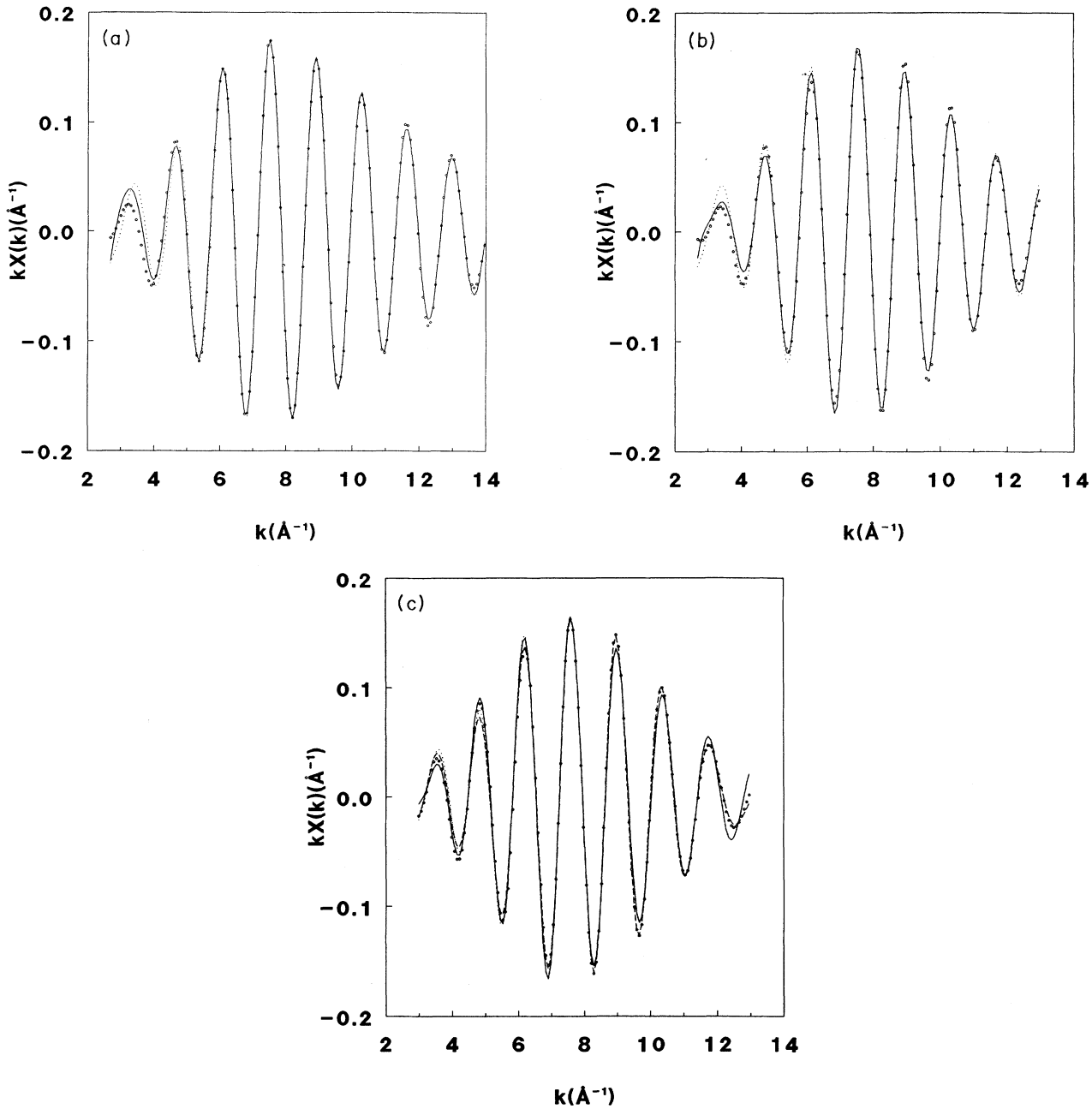

FIG. 3. The least-squares fit of $k\chi_c(k)$ experimental data (open circles) for neighboring shells about Mn allowing for the presence of large disorder. Solid line: C_{2j}, C_{3j}, and C_{4j} cumulants used for the two-shell fit, $j=1,2$. Dotted line: C_{2j}, C_{3j}, and C_{4j} cumulants used for the one-shell fit, $j=1$. Dashed line in (c) is obtained in the framework of the one-shell model using C_2, C_3, C_4, C_5, C_6, C_7, and C_8 cumulants. Their values are 7.0×10^{-3} Å^2, 60.0×10^{-3} Å^3, 43.0×10^{-3} Å^4, 1.9×10^{-5} Å^5, 0.3×10^{-5} Å^6, -0.1×10^{-6} Å^7, and 0.5×10^{-8} Å^8, respectively. The residual value for this fit was 9.8×10^{-3}. (a) The MnAs film with NiAs structure. (b) The $In_{0.88}Mn_{0.12}As$ film grown at 280 °C substrate temperature. (c) The $In_{0.88}Mn_{0.12}As$ film grown at 210 °C substrate temperature.

TABLE III. Curve-fitting results with a model allowing higher-order cumulants in the effective radial distribution of atoms in the shells due to the presence of disorder. The distances R are in units of Å. σ^2 in the Debye-Waller factors are in units of 10^{-3} Å^2. Cumulants C_2, C_3, and C_4 are in units of 10^{-3} Å^2, 10^{-5} Å^3, and 10^{-5} Å^4, respectively. Coordination numbers were fixed at their crystallographical values given in Table I. p is the relative fractional occupation parameter. r is the residual value of the fit $\times 10^{-3}$. Central atom: Mn. An asterisk indicates that the parameter's value was fixed during fitting. F.E. means fit errors.

	Neighboring shells										
	As(NiAs-like)				Mn(NiAs-like)				As(zinc blende)		
	R	C_2	C_3	C_4	R	C_2	C_3	C_4	σ^2	p(%)	r
MnAs											
	2.571*	1.9	1.1	0.8							17.8
	2.571*	1.6	2.1	0.2	2.845*	19	140	−13			5.7
F.E.		0.6	8	1.1		20	1200	45			
$In_{1-x}Mn_xAs$	$T_s=280$°C										
	2.55	2.1	−2.4	−1.0							10.4
	2.57	1.3	7.6	−2.8	2.83	28	11	22			6.0
	2.57	1.3	7.6	−2.8	2.83	28	11	22	0.2	0.4	6.0
F.E.	0.013	0.6	9	1.7	0.22	30	1200	34	7	3	
$In_{1-x}Mn_xAs$	$T_s=210$°C										
	2.58	1.3	26.0	−4.8							14.0
	2.58	1.3	26.0	−4.8	2.83*	26	2220	−87			9.8
	2.58	1.3	26.0	−4.8	2.83*	26	2220	−87	0.04	1.5	10.7
F.E.	0.013	0.8	13	2.6		30	5000	100	7	3	

proved by assuming an effective single shell of As nearest neighbors and using higher-order cumulants. This is borne out in our analysis, as shown by the dashed curve in Fig. 3(c), where a one-shell model with more cumulants (up to C_8) indeed improves the fit significantly (residual value decreased by a factor of 3). This improvement is especially visible in the higher-k regime ($k > 7$ Å).

Further expansion of the model to include some fraction p of Mn in the $In_{1-x}Mn_xAs$ alloy with zinc-blende structure with a 2.55–2.62 Å nearest-neighbor distance does not improve the fits in both the high- and low-growth-temperature samples, and this leads to unphysical, very small values of σ^2 in the Debye-Waller factors. Again, one can conclude that the p parameter is small and may be below the detection limit of our XAFS experiment.

C. Distant-shell analysis

Besides the dominant main peak which originated from the first two or three shells, some smaller peaks are also observed in the magnitude of the Fourier transform. Analysis of these features was hindered due to the relatively low signal-to-noise ratio of data in the higher-r domain. Other difficulties are posed by the unknown k dependence of the photoelectron mean free path and possible presence of multiple scattering. The effect of the former appears to be negligible in the first shell;[6] however, this assumption may not be justified for the higher-order neighbor shells. For simplicity's sake, and due to the limited degree of freedom of curve fitting in further analysis, we have neglected the k dependence of the mean free path.

The contribution due to distant shells ($3 < r < 5$ Å) was extracted from the data by subtracting χ_2 from χ_1 and transforming the difference signal to r space. The χ_i is the filtered XAFS function obtained by means of a window function w_i and backtransformed to k space. Window functions w_1 and w_2 were selected as shown in Fig. 1. The obtained results are shown in Fig. 4. By inspecting the obtained difference XAFS signals shown in this figure, one can reach the conclusion that the spectrum due to the high-growth-temperature sample is very similar to the MnAs spectrum with a reduced amplitude. However, the spectrum due to the low-growth-temperature sample is very different. A peak in the magnitude of Fourier transform at ~3.3 Å and characteristic contribution from Mn backscattering atoms to the real part of the Fourier transform has been observed for both the MnAs and the high-growth-temperature samples. These features can be ascribed to a shell with six Mn atoms at ~3.71Å from the central Mn atom. They are absent in the difference-spectrum transform obtained for the low-growth-temperature sample. Instead, a peak in the magnitude and a characteristic contribution from In backscattering atoms to the real part of the Fourier transform at ~4.1 Å appear. These features are attributed to a shell with 12 In atoms nominally at 4.278 Å expected in the zinc-blende structure. The fitting results gave rise to a shell of six Mn at 3.71±0.02-Å and a shell of 12 In at 4.25±0.02-Å distance for high- and low-growth-temperature samples, respectively (see Table IV).

The absence of a peak due to the Mn shell at 3.71 Å in the XAFS spectrum of the low-growth-temperature sample can be explained either by the large disorder or total lack of this shell. On the other hand, a peak at ~4.1 Å

TABLE IV. Curve-fitting results for distant shells with a model assuming small Gaussian disorder obtained for the high- and low-growth-temperature sample. The distance R is in units of Å. σ^2 in the Debye-Waller factor is in units of 10^{-3} Å^2. N denotes the number of neighbors in a shell. Central atom: Mn. F.E. means fit errors. E.E. means estimated experimental errors.

	Neighboring shells						
	Mn			In			Residual
	R	N	σ^2	R	N	σ^2	($\times 10^{-3}$)
$In_{1-x}Mn_xAs$		$T_s=280$ °C					
	3.71	5.2	4.6				6.4
F.E.	0.02	1.0	4				
E.E.	0.02	1.2	5				
$In_{1-x}Mn_xAs$		$T_s=210$ °C					
				4.25	12.1	13	6.5
F.E.				0.02	1.8	10	
E.E.				0.02	2.4	15	

produced by the more distant shell of 12 In atoms at 4.25 Å is visible in either the magnitude and real part of the Fourier transform. These results can be reconciled if one assumes that in the low-growth-temperature sample the central Mn atom has six As neighbors forming a highly disordered first-neighbor shell at the average distance 2.58 Å. There is a possibility that the second-neighbor Mn shell exists with even larger disorder. This shell consists possibly of two Mn atoms at approximate distance 2.83 Å. The third-neighbor shell is well ordered and is formed by 12 In atoms at 4.25 Å, recovering the zinc-blende structure. We can conclude that the Mn atoms are embedded in the form of locally disordered centers in the InAs matrix. The radius of these Mn centers is smaller than 3 Å.

The absence of the 4.278-Å peak in the magnitude of the Fourier transform obtained for the high-growth-temperature film also confirms the low (below a few percent) concentration or absence of the zinc-blende components in this sample, as discussed in Sec. III A.

D. Near-edge-structure analysis

We have also investigated the near-edge structure of $In_{1-x}Mn_xAs$ and MnAs samples at the Mn K edge (see Fig. 5). The main features in this spectral regime are due to $1s \rightarrow 4p$ and $1s \rightarrow 3d$ transitions. The dipole-allowed $1s \rightarrow 4p$ transition gives rise to the dominant peak in the

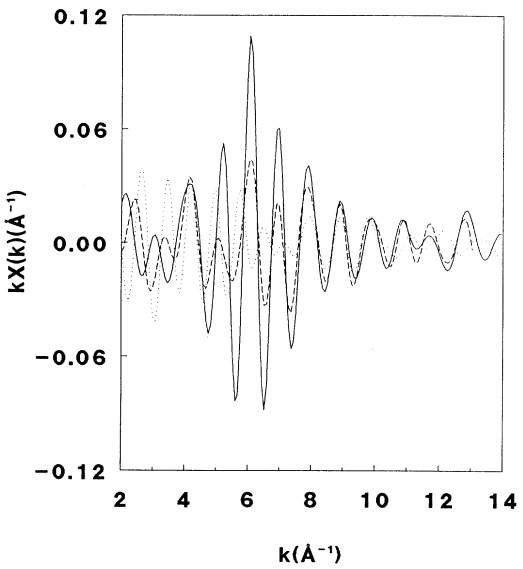

FIG. 4. The contribution due to distant shells ($3 < r < 5$ Å) extracted from the data by subtracting χ_2 from χ_1. The χ_i is the filtered XAFS function obtained by means of a window function w_i and backtransformed to k space. Window functions w_1 and w_2 were selected as shown in Fig. 1. The MnAs film with NiAs structure: solid line. The $In_{0.88}Mn_{0.12}As$ film grown at 280 °C substrate temperature: dashed line. The $In_{0.88}Mn_{0.12}As$ film grown at 210 °C substrate temperature: dotted line.

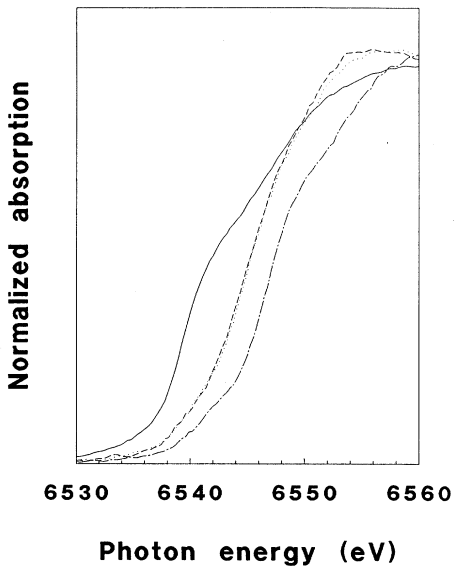

FIG. 5. The near-edge-structure spectra at the Mn K edge. Chain line: the MnAs film with NiAs structure. Dotted line: the $In_{0.88}Mn_{0.12}As$ film grown at 280 °C substrate temperature. Broken line: the $In_{0.88}Mn_{0.12}As$ film grown at 210 °C substrate temperature. Solid line: the metallic manganese.

near-edge structure. The primarily quadrupole $1s \rightarrow 3d$ transition is expected at lower energy. Its intensity is always significantly lower than that of the dipole-allowed transition. However, it can be strongly influenced by the degree of hybridization with $4p$ orbitals, which in turn depends on the nearest-neighbors coordination number, their nature and SRO, as was demonstrated for Fe compounds.[14,15] It is well known that the locations of the absorption thresholds shift to higher energy with increasing valency. This effect can be clearly observed in the spectra shown in Fig. 5. The metallic Mn has its absorption threshold for the $1s \rightarrow 4p$ transition at 6539 eV. The threshold for the same process in formally trivalent Mn in the MnAs sample is observed at 6547 eV, i.e., at an energy higher by 8 eV. Between these two positions at 6545 eV the absorption thresholds due to the $1s \rightarrow 4p$ transitions in the low- and high-growth-temperature $In_{1-x}Mn_xAs$ films are observed. The $1s \rightarrow 3d$ transition for the MnAs sample appears at 6541 eV. Again, the shift toward lower energy by 2 eV is observed for both $In_{1-x}Mn_xAs$ samples, and these $3d$ features are located at 6539 eV. This finding can be explained by the chemical shift of the $1s$ core level, whose position is a function of the local charge, i.e., the higher the valency the lower the $1s$ level. The uniform shift by -2 eV of the $1s \rightarrow 4p$ and $1s \rightarrow 3d$ thresholds observed for $In_{1-x}Mn_xAs$ samples relative to the MnAs compound indicates that the Mn effective valency in both $In_{1-x}Mn_xAs$ films is similar and lower than $+3$.

Besides the shifts, no change in the intensities of the $4p$ and $3d$ features are observed. The virtually identical intensities of the $3d$ features in both the $In_{1-x}Mn_xAs$ films may indicate very similar average coordination of the majority of manganese atoms in these two samples.

IV. CONCLUSIONS

From our XAFS data analysis one can conclude that in the high-growth-temperature $In_{1-x}Mn_xAs$ sample Mn and As atoms tend to form clusters with the NiAs structure embedded in the InAs matrix. The nearest-neighbor shell of Mn consists of six As atoms, the second and the third shells of two and six Mn atoms, respectively. Only a very small fraction of Mn atoms, below the detection limit of our XAFS measurements, may substitute for In in the zinc-blende structure and be fourfold coordinated by neighboring As atoms. No significant disorder is observed.

The local structure about Mn in the low-growth-temperature $In_{1-x}Mn_xAs$ film is quite different. The majority of Mn forms highly disordered sixfold-coordinated Mn-As centers. The presence of disorder in these centers was established by the breaking down of the approximation of Gaussian pair distribution, and the lack of observable backscattering signal due to the Mn shell at 3.71 Å which was detected in the high-growth-temperature sample. These centers appear to be located at the group-III sublattice sites of the InAs matrix, as indicated by the presence of an XAFS signal originating from a distant shell with 12 In atoms at 4.25 Å. A small number of Mn atoms may substitute for In atoms and be fourfold coordinated by the As nearest neighbors.

The results obtained in this work are qualitatively consistent with XRD and magnetization results. The high-growth-temperature $In_{1-x}Mn_xAs$ sample exhibited ferromagnetic behavior similar to MnAs and the presence of a second phase in XRD. Based on the XAFS results, this can be explained by the presence of small clusters of MnAs with the NiAs structure in the InAs matrix.

The low-growth-temperature $In_{1-x}Mn_xAs$ film was predominantly paramagnetic, and no foreign phase was detected in XRD as compared to that of the high-growth-temperature sample. This is consistent with the picture emerging from the XAFS investigation, through which we found that the majority of Mn atoms appears to form very small centers (with a radius below 3 Å), most likely limited to the central Mn and six neighboring As atoms with disordered bonds. The actual positions of the neighboring As atoms cannot be determined from the present XAFS experiment. The absence of ferromagnetic ordering can be explained either by the high disorder associated with the Mn-Mn bonds or by the complete lack of Mn neighboring shells around the central Mn atoms.

The effective valency of the majority of Mn atoms in the $In_{1-x}Mn_xAs$ films as deduced from the near-edge-structure investigations is the same for both the high- and low-growth-temperature samples. The apparent valency is lower than $+3$. The average coordination of the majority of Mn atoms inferred from the near-edge-structure investigations appears to be the same for both films. This result is also in agreement with the virtually identical sixfold-coordinated nearest-neighbor environment inferred from the XAFS analysis.

ACKNOWLEDGMENTS

We gratefully acknowledge T. Penney and S. von Molnar for their fruitful discussions on magnetism and local structures of these samples. The research at the State University of New York at Buffalo was supported by DOE under Grant No. DE-FG02-87ER45283. The X3 beamline was supported by DOE under Grant No. DE-FG02-91ER45231. The work at IBM was supported in part by the Army Research Office.

[1]H. Munekata *et al.*, Phys. Rev. Lett. **63**, 1849 (1989).
[2]H. Munekata *et al.*, J. Vac. Sci. Technol. B **8**, 176 (1990).
[3]H. Ohno *et al.*, J. Appl. Phys. **69**, 6103 (1991).
[4]H. Munekata, H. Ohno, R. R. Ruf, R. J. Gambino, and L. L. Chang, J. Cryst. Growth **11**, 1011 (1991).
[5]S. von Molnar *et al.*, J. Magn. Magn. Mater. **93**, 356 (1991).
[6]P. A. Lee, F. H. Citrin, P. Eisenberger, and B. M. Kincaid, Rev. Mod. Phys. **53**, 769 (1981); T. M. Hayes and J. B. Boyce, in *Solid State Physics,* edited by H. Ehrenreich, F. Seitz, and D. Turnbull (Academic, New York, 1982), Vol. 37, p. 173; E. A. Stern and S. M. Heald, in *Handbook on Synchrotron Radiation,* edited by E. E. Koch (North-Holland, New York,

1983), Vol. 1, p. 955; D. E. Sayers and B. A. Bunker, in *X-ray Absorption,* edited by D. C. Koningsberger and R. Prins (Wiley, New York, 1988), p. 211.

[7]J. Jaklevic, J. A. Kirby, M. P. Klein, A. S. Robertson, G. S. Brown, and P. Eisenberger, Solid State Commun. **23**, 679 (1977).

[8]B. L. Henke, P. Lee, T. J. Tanaka, R. L. Shimabukuro, and B. K. Fujikawa, At. Data Nucl. Data Tables **27**, 3 (1982).

[9]A. G. McKale, B. W. Veal, A. P. Paulikas, S.-K. Chan, and G. S. Knapp, J. Am. Chem. Soc. **110**, 3763 (1988).

[10]X-ray-diffraction peaks of the MnAs sample coincide reasonably well with the literature values of the MnAs with the NiAs phase.

[11]P. Eisenberger and G. S. Brown, Solid State Commun. **29**, 481 (1979).

[12]E. D. Crozier, J. J. Rehr, and R. Ingalls, in *X-ray Absorption,* edited by D. C. Koningsberger and R. Prins (Wiley, New York, 1988), p. 373.

[13]G. Bunker, Nucl. Instrum. Methods **207**, 437 (1983).

[14]A. L. Roe, D. J. Schneider, R. J. Mayer, J. W. Pyrz, J. Widom, and L. Que, Jr., J. Am. Chem. Soc. **106**, 1676 (1984).

[15]C. Y. Yang, S. M. Heald, J. M. Tranquada, Y. Xu, Y. L. Wang, and A. R. Moodebaugh, Phys. Rev. B **39**, 6681 (1989).